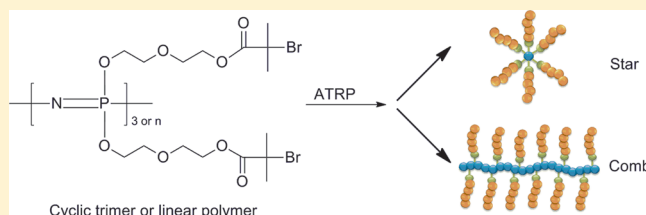


# Synthesis and Characterization of Brush-Shaped Hybrid Inorganic/Organic Polymers Based on Polyphosphazenes

Xiao Liu, Zhicheng Tian, Chen Chen, and Harry R. Allcock\*

Department of Chemistry, The Pennsylvania State University, University Park, Pennsylvania 16802, United States

**ABSTRACT:** A series of densely grafted star- and comb-shaped molecular brushes composed of polystyrene, poly(*tert*-butyl acrylate), and poly(*N*-isopropylacrylamide) were prepared by atom transfer radical polymerization (ATRP) using either cyclotriphosphazenes or polyphosphazenes as initiators. The initiators were prepared by the introduction of a free hydroxyl group into the side chains of a phosphazene cyclic trimer and polymer, followed by esterification with 2-bromopropionyl bromide. The grafting conditions were optimized for various monomers. The kinetics of the reaction were first-order with respect to the monomer concentration in both cyclotriphosphazene and polyphosphazene systems. The molecular weights of the resulting polymers were estimated by gel permeation chromatography (GPC). The side chains of the brush polymers were cleaved from the backbone and analyzed by GPC to confirm the synthesis of well-defined polymer brushes. Brushes based on poly(*tert*-butyl acrylate) were subjected to hydrolysis to yield negatively charged brushes. In addition, the lower critical solution temperature (LCST) of poly(*N*-isopropylacrylamide) brush polymers was measured by both dynamic light scattering (DLS) and differential scanning calorimetry (DSC), exhibiting a sharp phase transition at 33 °C. Furthermore, star- and comb-block copolymers with a hard polystyrene core and a soft poly(*tert*-butyl acrylate) shell were also synthesized.



## INTRODUCTION

Molecular brushes consisting of multiple polymer chains grafted onto a linear polymer are among the most intriguing macromolecular structures because they have unique chemical and physical properties.<sup>1–3</sup> Because of competing forces between the backbone and side chains, brush polymers usually adopt a cylindrical conformation. The densely grafted side chains repel each other, but their ability to move apart is hindered by the backbone, which confines the side chains to a cylindrical volume.<sup>4</sup> This leads to numerous distinctive properties of molecular brushes. The most important attribute of molecular brushes is their molecular segregation. For example, unlike linear polymers, the reversible conformational changes in response to external stimuli can be limited to the single molecule identified by atomic force microscopy.<sup>5,6</sup> In addition, steric repulsion between the side chains generates significant mechanical tension in the backbone which can be tuned by varying the grafting density, solvent quality, and the side chain length.<sup>7,8</sup> Furthermore, a stable unimolecular micelle of cylindrical shape formed from amphiphilic molecular brush copolymers cannot dissociate in aqueous solution, which is one of the major disadvantages associated with polymer micelles formed from amphiphilic linear polymers.<sup>9,10</sup>

Because of their nonspherical macromolecular geometries and lengths up to a few hundred nanometers, brush polymers have afforded numerous potential applications in nanoscience, such as molecular actuators,<sup>11</sup> templates for inorganic particles,<sup>9</sup> and as precursors for nanocapsules,<sup>12</sup> nanotubes,<sup>13</sup> and other carbon nanostructures.<sup>14</sup> Another prominent application of molecular brushes is in the biological field, due to the similar molecular structures of their natural counterparts known as

proteoglycans,<sup>15,16</sup> which are brushlike polyelectrolytes that consist of a protein backbone with carbohydrate side chains. Proteoglycans are found in a variety of places within the body and perform multiple biological functions such as cell signaling and cell surface protection,<sup>17</sup> shock absorption, lubrication,<sup>18,19</sup> and lung clearance.<sup>20</sup> Therefore, molecular brushes have been widely studied as synthetic counterparts for natural proteoglycans in order to better understand the architecture–property relationships, which could potentially lead to advances in biomedical applications.

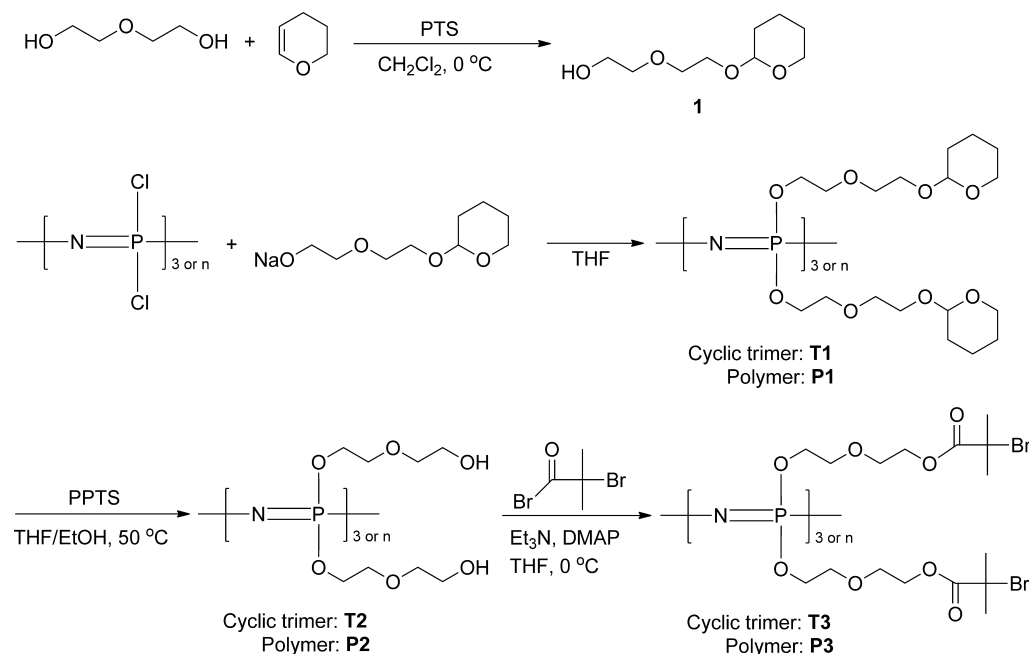
However, even though a considerable number of molecular brushes have been synthesized and studied, most of these brush polymers are built up from backbones based on carbon–carbon polymers, such as poly(styrene),<sup>21</sup> poly(methacrylate) derivatives,<sup>22,23</sup> polynorbornenes,<sup>24</sup> and poly(thiophene).<sup>25,26</sup> A further study of molecular brushes based on novel polymer backbones offers the opportunity to extend this field in novel ways. The construction of molecular brushes based on non-carbon backbones provides a means to elucidate the effect of the backbone on molecular conformation as well as the resulting chemical and physical properties. Also, the lack of biodegradability of most molecular brushlike materials limits their applications in biological areas, some of which require degradation after fulfilling a function in the human body and allowing renal excretion of the small molecule products.<sup>27</sup> The lengths of molecular brushes are usually up to hundreds of nanometers,<sup>9,11</sup> which is too large for direct renal excretion,

Received: November 28, 2011

Revised: January 5, 2012

Published: January 18, 2012

Scheme 1. Synthesis of Macroinitiators T3 and P3



since it has been shown that only linear polymers with molecular weights below 40 kDa, or  $\sim 5$  nm in diameter, are cleared readily through the renal system.<sup>27</sup> A possible solution to this specific problem is to design the backbone of molecular brush polymers to be biodegradable to release short side chain products, which are small enough to allow kidney-based excretion.

Polyphosphazenes provide a way to construct molecular brushes with a hydrolytically degradable backbone. Polyphosphazenes are hybrid organic–inorganic polymers that contain a flexible phosphorus–nitrogen backbone with various side groups, such as organic,<sup>16,28</sup> organometallic,<sup>29</sup> or inorganic units.<sup>30</sup> Thus, polyphosphazenes potentially offer advantages over other polymers for biomedical applications since the side groups can be changed easily by macromolecular substitution methods to target specific combinations of properties. In addition, polyphosphazenes can be designed to be hydrolyzable, in a way that liberates the side groups and converts the backbone to a pH-buffered mixture of phosphate and ammonia which can neutralize the acid degradation products from polyester segments.<sup>31,32</sup> The side groups can be selected to be biocompatible, the phosphate may be metabolized, and the ammonia, which is innocuous at low concentrations, can be excreted.<sup>31,32</sup>

The preparation of some molecular brushes based on polyphosphazenes with organic polymer grafts has been reported in earlier publications.<sup>29,33</sup> There are three main strategies for preparing such species. These are “grafting through” (the polymerization of macromonomers),<sup>34,35</sup> “grafting onto” (the addition of previously prepared side chains to a backbone),<sup>36,37</sup> and “grafting from” (the polymerization of side chains from a macroinitiator backbone).<sup>29,33,38</sup> By far, the largest effort to construct brushlike polyphosphazenes has been reported by Gleria and co-workers using the “grafting from” technique.<sup>29,39,40</sup> Their strategy was to use a poly(organophosphazene) with organic side groups that would generate free radical sites when treated with peroxides or when exposed to high-energy radiation. These radical sites then served as

initiation species for the free radical polymerization of vinyl-type monomers. However, one of the major drawbacks of this classical free radical polymerization process is the difficulty of controlling different structural parameters, including chemical composition, grafting density, degree of polymerization of side chains, and sequential grafting of second segments. In addition, a high concentration of radical species during free radical polymerization may cause intramolecular termination resulting in pendant macrocycles and even forming intermolecular coupling and macroscopic gelation.<sup>41</sup>

Controlled/living radical polymerization (CRP), especially atom transfer radical polymerization (ATRP), is a versatile route for the synthesis of well-defined polymers with predetermined molecular weights, narrow molecular weight distributions, various architectures, and useful end-functionalities.<sup>9,10,23,41</sup> Thus, ATRP has been widely used for complete control/design of the molecular architecture of brushes, producing unique and novel molecules.<sup>4,10,22</sup> More importantly, ATRP can maintain a low instantaneous concentration of radical species which necessarily limits termination events and avoids macroscopic gelation from intermolecular coupling. In fact, several researchers have explored the field of synthesis of hybrid materials based on polyphosphazenes by the ATRP technique.<sup>42–44</sup>

In this study, we report the preparation of nonlinear brushes with six-armed star architecture and comb structures through ATRP by using the starlike cyclotriphosphazene or a linear macroinitiator based on a polyphosphazene, with subsequent grafting-from various monomers as shown in Scheme 1. A series of six-armed star and comb brush polymers were synthesized, and their compositions were analyzed. Confirmation of the functionality of the resultant polymers has also been demonstrated. Star- and comb-block copolymers from multifunctional polymeric macroinitiators were also synthesized.

## EXPERIMENTAL SECTION

**Materials.** All reactions were carried out under a dry argon atmosphere using standard Schlenk line techniques. Tetrahydrofuran (EMD) and triethylamine (EMD) were dried using solvent

purification columns.<sup>45</sup> 3,4-Dihydro-2H-pyran (Acros), diethylene glycol (Sigma), *p*-toluenesulfonic acid monohydrate (Alfa Aesar), pyridinium *p*-toluenesulfonate (PPTS) (Aldrich), sodium hydride (Aldrich), 2-bromopropionyl bromide (Sigma), pentamethyldiethylenetriamine (PMDETA) (TCI), and copper(I) bromide (Sigma) were used as received. Styrene (Aldrich) and *tert*-butyl methacrylate (Aldrich) were stirred over calcium hydride for 2 days and distilled under vacuum. The distillates were stored at  $-54\text{ }^{\circ}\text{C}$  before use. *N*-Isopropylacrylamide was purified by recrystallization from hexane to remove the inhibitor and dried under vacuum. Tris[2-(dimethylamino)ethyl]amine ( $\text{Me}_6\text{-TREN}$ ) was synthesized according to a literature procedure.<sup>46</sup> Hexachlorocyclotriphosphazene (HCCTP) (Fushimi Pharmaceutical Co., Japan, or a Ningbo Chemical, China) was purified by recrystallization from hexanes and vacuum sublimation at  $50\text{ }^{\circ}\text{C}$ . Poly(dichlorophosphazene) was prepared by the thermal ring-opening polymerization of recrystallized and sublimed hexachlorocyclotriphosphazene in evacuated Pyrex tubes at  $250\text{ }^{\circ}\text{C}$ .<sup>47</sup>

**Equipment.**  $^1\text{H}$  and  $^{31}\text{P}$  NMR spectra were obtained using a Bruker AMX-360 NMR spectrometer, operated at 360 and 146 MHz, respectively.  $^1\text{H}$  NMR spectra were referenced to tetramethylsilane signals while  $^{31}\text{P}$  NMR chemical shifts were referenced to 85% phosphoric acid as an external reference, with positive shift values downfield from the reference. All chemical shifts are reported in ppm. Molecular weight distribution data were obtained using a Hewlett-Packard HP 1090 gel permeation chromatograph equipped with two Phenomenex Phenogel linear 10 columns and a Hewlett-Packard 1047A refractive index detector. The samples were eluted at  $1.0\text{ mL/min}$  with a  $10\text{ mM}$  solution of tetra-*n*-butylammonium nitrate in THF. The elution times were calibrated with polystyrene standards.

**Synthesis of Macroinitiators.** 2-[2-(Tetrahydropyranyloxy)ethoxy]ethanol (**1**). At  $-10\text{ }^{\circ}\text{C}$ , 3,4-dihydro-2H-pyran (21.3 g, 0.23 mol) was added over a period of 45 min to a mixture of 46 mg of *p*-toluenesulfonic acid (PTS) in 180 mL (1.89 mol) of diethylene glycol. The reaction mixture was stirred for 1 h at  $-10\text{ }^{\circ}\text{C}$  and then for 2 h at room temperature. The mixture was poured into 500 mL of 1 M  $\text{NaOH}_{(\text{aq})}$  and extracted with dichloromethane ( $5 \times 200\text{ mL}$ ). The combined organic layers were dried over  $\text{MgSO}_4$  and concentrated under vacuum. The crude product was distilled at reduced pressure. The colorless liquid product was obtained with yield of 30.7 g (70.0%).  $^1\text{H}$  NMR ( $\text{CDCl}_3$ ),  $\delta$ : 4.55 (t, OCHO, 1 H,  $J = 3.54\text{ Hz}$ ), 3.80–3.43 (m,  $\text{OCH}_2$ , 10 H), 1.72–1.44 (m,  $\text{CH}_2$ , 6 H).

Hexakis[2-[2-(tetrahydropyranyloxy)ethoxy]ethoxy]cyclo-triphosphazene (**T1**). A THF solution (50 mL) of hexachlorocyclotriphosphazene (2.0 g, 5.75 mmol) was added dropwise to a THF (50 mL) suspension of the sodium salt of **1**, prepared from 2-[2-(tetrahydropyranyloxy)ethoxy]ethanol (7.66 g, 40.3 mmol) and sodium hydride (1.73 g, 43.1 mmol). The solution was stirred for 48 h at reflux. THF was removed by rotary evaporation, and the mixture was redissolved in dichloromethane. The mixture was transferred to a separatory funnel and extracted consecutively with deionized water ( $100\text{ mL} \times 3$ ),  $\text{NaHCO}_{3(\text{aq})}$  ( $100\text{ mL} \times 3$ ), and deionized water ( $100\text{ mL} \times 3$ ). The organic phase was dried over  $\text{MgSO}_4$  overnight then filtered, and the solvent was removed by rotary evaporation. The crude product was purified by silica column chromatography with an eluent of hexane/ethyl acetate (4:6). After evaporation of the eluent, a colorless oil was obtained with a yield of 6.2 g (84.9%).  $^1\text{H}$  NMR ( $\text{CDCl}_3$ ),  $\delta$ : 4.60 (t, OCHO, 1 H,  $J = 3.44\text{ Hz}$ ), 4.05–3.50 (m,  $\text{OCH}_2$ , 10 H), 1.83–1.51 (m,  $\text{CH}_2$ , 6 H).  $^{31}\text{P}$  NMR ( $\text{CDCl}_3$ ),  $\delta$ : 18.5 (s).

Hexakis[2-(2-hydroxyethoxy)ethoxy]cyclo-triphosphazene (**T2**). Hexakis[2-[2-(tetrahydropyranyloxy)ethoxy]ethoxy]cyclo-triphosphazene (**T1**) (1 g, 0.79 mmol) was first dissolved in dichloromethane (5 mL), and a solution of pyridinium-*p*-toluenesulfonate (PPTS) (0.06 g, 0.24 mmol) in absolute ethanol (50 mL) was added slowly. The solution was heated at  $50\text{ }^{\circ}\text{C}$  for 1 day. The ethanol was removed by rotary evaporation and redissolved in deionized water. The crude product was purified by means of a LH 20 column. Yield: 0.2 g, 33.1%.  $^1\text{H}$  NMR ( $\text{D}_2\text{O}$ ),  $\delta$ : 4.17 (t,  $\text{POCH}_2\text{CH}_2\text{O}$ , 2 H,  $J = 4.43$ ), 3.80–3.66 (m,  $\text{OCH}_2$ , 6 H).  $^{31}\text{P}$  NMR ( $\text{D}_2\text{O}$ ),  $\delta$ : 18.4 (s).

Hexakis[2-[2-(2-bromoisobutyryloxy)ethoxy]ethoxy]cyclo-triphosphazene (**T3**). Hexakis[2-(2-hydroxyethoxy)ethoxy]cyclo-triphosphazene (**T2**) (1 g, 1.30 mmol) was placed in a 100 mL Schlenk flask with THF (50 mL), triethylamine (1.2 g, 11.8 mmol), and 4-(dimethylamino)pyridine (DMAP) (0.48 g, 3.90 mmol). A solution of 2-bromopropionyl bromide (2.7 g, 11.8 mmol) in 20 mL of THF was added dropwise to the reaction mixture at  $0\text{ }^{\circ}\text{C}$  in an ice bath. The mixture was stirred for 2 days and allowed to warm to room temperature. The solvent was removed by rotary evaporation, and the residue was redissolved in dichloromethane. The mixture was transferred to a 200 mL separatory funnel and extracted consecutively with deionized water ( $100\text{ mL} \times 3$ ),  $\text{NaHCO}_{3(\text{aq})}$  ( $100\text{ mL} \times 3$ ), and deionized water ( $100\text{ mL} \times 3$ ). The organic phase was dried over  $\text{MgSO}_4$  and then filtered, and the solvent was removed by rotary evaporation. The crude product was passed through a silica gel column with an eluent of dichloromethane and ethyl acetate (5:3). The solvent was removed, and the resulting light yellow oil was dried under vacuum at room temperature. Yield: 0.41 g (27.0%).  $^1\text{H}$  NMR ( $\text{CDCl}_3$ ),  $\delta$ : 4.17 (t,  $\text{POCH}_2\text{CH}_2\text{O}$ , 2 H), 3.96 (t,  $\text{CH}_2\text{OC}(\text{O})$ , 2 H,  $J = 4.86\text{ Hz}$ ) 3.67–3.61 (m,  $\text{OCH}_2$ , 4 H), 1.85 (s,  $\text{C}(\text{Br})\text{CH}_3$ , 6 H).  $^{31}\text{P}$  NMR ( $\text{CDCl}_3$ ),  $\delta$ : 18.4 (s).

Poly[bis[2-[2-(tetrahydropyranyloxy)ethoxy]ethoxy]phosphazene] (**P1**). A THF solution (150 mL) of poly(dichlorophosphazene) (3.0 g, 25.9 mmol) was added to a THF (150 mL) suspension of the sodium salt of **1**, prepared from 2-[2-(tetrahydropyranyloxy)ethoxy]ethanol (12.3 g, 64.7 mmol) and sodium hydride (2.90 g, 72.5 mmol). The reaction solution was stirred for 48 h at reflux. The polymer solution was concentrated by rotary evaporation, and the residue was poured into water to obtain the precipitate of the polymeric product, which was further purified by repeated precipitation three times into water and *n*-hexane. The pure product was dried under vacuum to yield a yellow adhesive solid: 8.7 g (74.5%).  $^1\text{H}$  NMR ( $\text{CDCl}_3$ ),  $\delta$ : 4.60 (br, s, OCHO, 1 H), 4.04–3.49 (m,  $\text{OCH}_2$ , 10 H), 1.84–1.50 (m,  $\text{CH}_2$ , 6 H).  $^{31}\text{P}$  NMR ( $\text{CDCl}_3$ ),  $\delta$ :  $-7.85$  (s).  $M_n = 165\,200$ , PDI = 3.8.

Poly[bis[2-(2-hydroxyethoxy)ethoxy]phosphazene] (**P2**). Poly[bis[2-[2-(tetrahydropyranyloxy)ethoxy]ethoxy]phosphazene] (**P1**) (9.61 g, 22.7 mmol) was first dissolved in dichloromethane (50 mL), and absolute ethanol (200 mL) was added slowly with pyridinium *p*-toluenesulfonate (0.57 g, 2.27 mmol). The solution was stirred at  $50\text{ }^{\circ}\text{C}$  for 3 days. The polymeric product was purified by dialysis against methanol for 4 days. An adhesive yellow product was obtained with yield of 4.86 g (50.2%).  $^1\text{H}$  NMR ( $\text{D}_2\text{O}$ ),  $\delta$ : 4.19 (br, s,  $\text{POCH}_2\text{CH}_2\text{O}$ , 2 H), 3.78–3.66 (m,  $\text{OCH}_2$ , 6 H).  $^{31}\text{P}$  NMR ( $\text{D}_2\text{O}$ ),  $\delta$ :  $-5.65$  (s).

Poly[bis[2-[2-(2-bromoisobutyryloxy)ethoxy]ethoxy]phosphazene] (**P3**). Poly[bis[2-(2-hydroxyethoxy)ethoxy]phosphazene] (**P2**) (4.86 g, 19 mmol) was placed into a 100 mL Schlenk flask with DMF (30 mL), triethylamine (5.78 g, 57.1 mmol), and 4-(dimethylamino)pyridine (2.32 g, 19.0 mmol). A solution of 2-bromopropionyl bromide (13.1 g, 57.1 mmol) in 10 mL of DMF was added dropwise to the reaction mixture at  $0\text{ }^{\circ}\text{C}$  in an ice bath. The reaction mixture was stirred overnight and allowed to warm to room temperature. The solvent was removed by rotary evaporation, and the residue was redissolved in methanol and dialyzed against methanol for 3 days to remove the impurities. The solvent was removed, and the resulting adhesive yellow product was dried under vacuum at room temperature. Yield: 7.46 g (71.0%).  $^1\text{H}$  NMR ( $\text{CDCl}_3$ ),  $\delta$ : 4.17 (br, s,  $\text{POCH}_2\text{CH}_2\text{O}$ , 2 H), 4.06 (br, s,  $\text{CH}_2\text{OC}(\text{O})$ , 2 H) 3.74–3.67 (m,  $\text{OCH}_2$ , 4 H), 1.92 (s,  $\text{C}(\text{Br})\text{CH}_3$ , 6 H).  $^{31}\text{P}$  NMR ( $\text{CDCl}_3$ ),  $\delta$ :  $-7.80$  (s).  $M_n = 88\,500$ , PDI = 2.06.

**Polymerization.** A typical polymerization was as follows: Polymeric macroinitiator **P3** (0.216 g, 0.78 mmol initiator centers), *tert*-butyl acrylate (20 g, 0.156 mol), and pentamethyldiethylenetriamine (PMDETA) (0.135 g, 0.78 mmol) were placed in a 50 mL Schlenk flask and sparged with nitrogen for 30 min. Anisole (0.5 mL) was used as an internal standard. Afterward, deoxygenated copper(I) bromide (0.056 g, 0.39 mmol) and copper(II) bromide (4.4 mg, 0.02 mmol) were added. Approximately 0.2 mL of solution was removed, and the nitrogen-filled flask was heated at  $90\text{ }^{\circ}\text{C}$  under nitrogen. Periodically, additional 0.2 mL aliquots were removed to analyze the

conversion and molecular weight by  $^1\text{H}$  NMR and GPC. The polymerization was terminated after 34.5 h at conversion 19.9% and was quenched by liquid nitrogen. The reaction mixture was then dissolved in dichloromethane and passed through a short alumina column to remove the copper catalyst. The polymer was purified by precipitation into cold methanol/water (4:1). Yield: 1.73 g (15.5%) of isolated polymer. The polymerization conditions of all other monomers are listed in Table 1.

**Table 1. Characterization Data for Initiators**

entry	$^{31}\text{P}$ NMR (ppm)	$M_n$	PDI	RU
T1	18.5	765.6		
T2	18.4	1270.3		
T3	18.4	1659.5		
P1	-7.8	165200	3.8	390
P2	-5.6	<i>a</i>		
P3	-7.8	88500	2.06	177

<sup>a</sup>P2 did not dissolve in THF.

**Star- and Comb-Polystyrene-block-poly(*tert*-butyl acrylate) (sPS-*b*-PtBuA and cPS-*b*-PtBuA).** A typical polymerization procedure is as follows: star-polystyrene (sPS) (0.2 g, 0.066 mmol initiator centers), *tert*-butyl acrylate (5.93 g, 46.3 mmol), and PMDETA (0.023 g, 0.132 mmol) were placed into a 20 mL Schlenk flask and sparged with nitrogen for 30 min. Deoxygenated copper(I) bromide (9 mg, 0.066 mmol) and copper(II) bromide (0.74 mg, 0.0033 mmol) were then added. The flask was heated at 90 °C under nitrogen. The polymerization was terminated after 24 h at a conversion of 61.6% and was quenched by liquid nitrogen. The reaction mixture was dissolved in dichloromethane and was passed through a short alumina column to remove the copper catalyst. The polymer was purified by precipitation into cold methanol/water (4:1) Yield: 2.5 g of isolated polymer.

**Solvolysis of Brush Polymers.** The side chains of star-poly(*tert*-butyl acrylate) (sPtBuA) and comb-poly(*tert*-butyl acrylate) (cPtBuA) were cleaved in the similar manner. Typically, 0.1 g of polymer (sPtBuA or cPtBuA) was dissolved in 5 mL of THF in a 50 mL Schlenk flask. *n*-Butanol (18 mL) was added. After the addition of 8 drops of concentrated sulfuric acid, the mixture was heated to 90 °C for 19 days. The solvent was removed under vacuum, and the remaining polymer was dissolved in dichloromethane and precipitated into cold methanol/water (4:1). The resultant polymer was dried under vacuum and analyzed by GPC.

The side chains of star-polystyrene (sPS) and comb-polystyrene (cPS) were cleaved in the similar manner. In a typical reaction, 0.1 g of polymer (sPS or cPS) was dissolved in 20 mL of THF in a 50 mL Schlenk flask, followed by the addition of 5 mL of 1 M KOH ethanol solution. The mixture was heated to 90 °C for 12 days. The solvent was removed by rotary evaporation. The crude product was redissolved in dichloromethane, extracted with deionized water, and dried over  $\text{MgSO}_4$ . After precipitation in methanol, the resultant polymer was analyzed by GPC.

**Deprotection of Star-Poly(*tert*-butyl acrylate) (sPtBuA) and Comb-Poly(*tert*-butyl acrylate) (cPtBuA).** Star-poly(acrylic acid) (sPAA) and comb-poly(acrylic acid) (cPAA) were prepared by hydrolysis of the *tert*-butyl esters of sPtBuA and cPtBuA following a literature method.<sup>48</sup> A typical procedure is as follows: sPtBuA (0.2 g) and iodotrimethylsilane (0.62 g, 3.12 mmol) were allowed to react in 15 mL dry dichloromethane under nitrogen for 1 day. The volatiles were then evaporated. After redissolving the mixture in methanol, the crude product was dialyzed against methanol for 2 days. The solvent was removed by rotary evaporation and dried at room temperature under vacuum overnight. Yield: 0.06 g.

**Determination of Lower Critical Solution Temperature of Comb-Poly(*N*-isopropylacrylamide) (cPNPA).** The lower critical solution temperature (LCST) of comb-poly(*N*-isopropylacrylamide) (cPNPA) was evaluated by dynamic light scattering (DLS) using a particle size analyzer (Zetasizer Nano S, Malvern Instruments Ltd.) with a scattering angle of 90° and a thermostatically controlled cell having a

heating rate of 1 °C min<sup>-1</sup>. Aqueous samples with a concentration of 2 mg/mL were filtered through a 0.45  $\mu\text{m}$  syringe filter before measurement of particle size for each sample. Also, the LCST was determined by differential scanning calorimetry (DSC) with a TA Instruments Q10 and a heating rate of 10 °C/min and a sample size of ca. 10 mg.

## RESULTS AND DISCUSSION

**Initiator Syntheses.** In this work, the “graft-from” approach was used to construct both star-shaped and comb-shaped brush polymers. For this purpose, initiators T3 and P3 were synthesized as illustrated in Scheme 1 using hexachlorocyclotriphosphazene (T1) or poly(dichlorophosphazene) (P1) as starting materials. As a representative example, the following pathways were involved in the preparation of initiator P3. Diethylene glycol was monoprotected by dihydropyran to yield compound 1. The sodium salt of 1 was allowed to react with poly(dichlorophosphazene) to produce polymer P1. The singlet resonance at -7.85 ppm in the  $^{31}\text{P}$  NMR spectrum suggested complete chlorine replacement. In the deprotection of the pyranil moiety, the polymer P1 solution in THF/ethanol was treated at 50 °C in the presence of pyridinium *p*-toluenesulfonate to yield polymer P2. The completion of deprotection was confirmed by the  $^1\text{H}$  NMR spectrum with the total disappearance of the resonances at 4.60 ppm and between 1.84 and 1.50 ppm, which were due to pyranil groups.

The macroinitiator P3 was synthesized by esterification of polymer P2 with 2-bromopropionyl bromide. The  $^1\text{H}$  NMR spectrum indicated 100% esterification of hydroxyl groups from the ratio between the methylene group at 4.17 ppm (2H) and the methyl groups at 1.92 ppm (6H). The initiator T3 was synthesized by a similar approach. Characterization data for the initiators are summarized in Table 1. Both of the initiators were used to induce polymerization of various monomers.

**Polymerization.** A series of star- and comb-shaped brushes were synthesized by grafting styrene, *tert*-butyl acrylate, and *N*-isopropylacrylamide from the aforementioned initiators (T3 and P3) by controlled atom transfer radical polymerization (ATRP) as illustrated in Scheme 2. Because the initiating groups remain at the ends of the grafted side chains, it was possible to extend the side chains in a well-defined manner.

**Synthesis of Star-Shaped Brush Polymers.** For each of the monomers studied, conditions were developed using T3 as an initiator, which provided linear first-order kinetic plots typical of a controlled living polymerization (Table 2). Figure 1a shows the linear relationships of  $\ln([M]_0/[M])$  vs time for these three monomers. This means that the concentration of growing radicals is constant during the polymerization in all systems, confirming the first-order in monomer concentration kinetics. However, the molecular weight vs time plot shown in Figure 1b illustrates marked deviations from the theoretical value calculated from the conversion of monomer in Table 2, which is approximately twice as high as the molecular weight measured by GPC (Table 2). For a controlled living polymerization the observed molecular weight should coincide with the theoretical value. The deviation of molecular weight from the theoretical value may be due to the highly compact nature of the polymers, which results in lower hydrodynamic volumes of star brush polymers and does not correspond well to the linear standards.<sup>49</sup>

During optimization of the ATRP of *tert*-butyl acrylate at 90 °C, cross-linking occurred when using higher concentrations of catalyst relative to initiator or lower monomer-to-initiator

Scheme 2. Graft of Different Monomers from Initiators T3 and P3

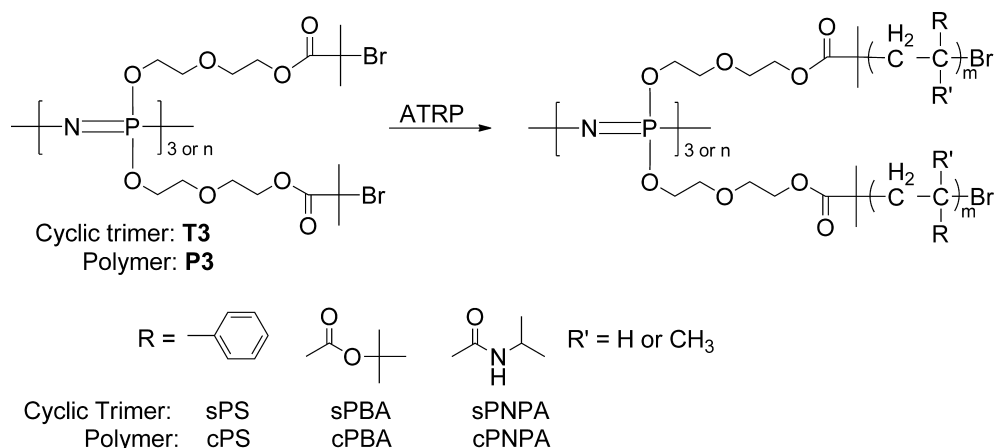


Table 2. Reaction Conditions for Grafting of Different Monomers from Initiator T3 and P3

entry	M	[M]:[I]:[CuBr]:[CuBr <sub>2</sub> ]:[ligand]	temp (°C)	time (h)	conv (%)	M <sub>n</sub> (PDI)		
						GPC <sup>a</sup>	conv <sup>b</sup>	cleavage <sup>c</sup>
sPS	Sty	1200:1:3:0.15:6	105	31.5	38.3	27 600 (1.22)	49 200	19 700
sPBA	BA	1200:1:3:0.15:6	90	13.5	61.7	45 700 (1.10)	96 600	53 000
sPNPA	NPA	1200:1:3:0.15:6	55	25	15.4	20 400 (1.35)	22 800	
cPS	Sty	400:1:2:0.1:1	105	40	22.4	200 300 (1.94)	1 903 700	862 100
cPBA	BA	400:1:2:0.2:1	90	34.5	19.9	125 700 (1.38)	1 749 600	2 086 300
cPNPA	NPA	400:1:2:0.1:1 <sup>d</sup>	50	96	5.2	173 900 (1.79)	1 349 000	

<sup>a</sup>Measured by GPC calibrated by linear polystyrene standards. <sup>b</sup>Calculated from conversion measured by NMR. <sup>c</sup>Calculated from cleaved side chains. <sup>d</sup>Reaction was conducted in methanol/DMF (10 mL/7 mL), and the ligand is Me<sub>6</sub>TREN.

ratios. Even when the ratio of monomer-to-initiator increased to 150 to 1, cross-linking was still detected. One consequence of using radical polymerization to grow the side chains from the backbone is that radical–radical coupling must be significantly suppressed. When the concentration of the active species is too high, radical coupling resulted in aggregates of stars, the appearance of a high molecular weight shoulder on the GPC traces, and ultimately cross-linking.<sup>50,51</sup> The results showed that cross-linking can be significantly suppressed when the monomer-to-initiator ratio is increased to 200 to 1.

The temperature should also be carefully controlled in order to obtain well-defined molecular structures. For example, it has been reported that, in some cases, ATRP of *N*-isopropylacrylamide in grafting reactions when heated or at room temperature may result in gel-like products due to cross-linking.<sup>25</sup> However, no cross-linking was detected in the present reactions either at room temperature or when heated. In contrast, increased temperature (50 °C) is necessary to improve the grafting efficiency of *N*-isopropylacrylamide.

Also, a sufficiently low active species concentration, which is 50 mol % relative to initiator, was used in order to avoid cross-linking and obtain well-defined molecular brushes with monomodal and narrow molecular weight distributions even at high monomer conversions. In addition, the deactivation species CuBr<sub>2</sub> (2.5 mol %) was added to avoid its spontaneous formation in situ by radical termination. This established better control by anticipation of the persistent radical effect.<sup>52</sup> Therefore, in every case, the graft polymerization of each monomer was well controlled, and this resulted in the synthesis of polymers with low polydispersity (Figure 1c). The absence of termination reactions from recombination reactions is indicated by the absence of a small shoulder in the high

molecular weight portion of the GPC trace for both sPS and sPBA (Figure 2).

**Synthesis of Comb-Shaped Brush Polymers.** Similarly, comb-shaped brush polymers were synthesized by grafting styrene, *tert*-butyl acrylate, and *N*-isopropylacrylamide from the P3 macroinitiator as illustrated in Scheme 2. As in the synthesis of the star-shaped brush polymers, Figure 3 shows linear first-order kinetic plots typical of a controlled living polymerization, which indicates conservation of radicals throughout the reaction of each monomer. However, a significant difference in polymerization rate was found when compared with the star-shaped brush system. These differences are apparent from the comparison in Figure 4, especially between the polymerization of styrene and *tert*-butyl acrylate from T3 and P3 initiators. In general, the polymerization rate in the comb–brush system is much slower than for the star–brush system. This is probably due to the more sterically hindered conformation of macroinitiator P3. Thus, the presence of adjacent polymer chains in comb–brush polymers may hinder polymer chain growth from the beginning. The star–brush system may also suffer from the same problem, but the relatively wide-open core structure will allow a much faster polymerization rate than the comb–brush system. Another specific example to illustrate the steric hindrance effect is the polymerization rate of styrene and *tert*-butyl acrylate in the same system. For example, sPBA has higher polymerization rate than sPS in star–brush reactions in the cyclotrimeric system (T3). This is probably due to the difference in reactivity among the different monomers. However, nearly identical polymerization rates of these two monomers were found in the comb–brush system (Figure 4), probably because the reactivity difference between styrene and *tert*-butyl acrylate is dominated by the steric hindrance effect,

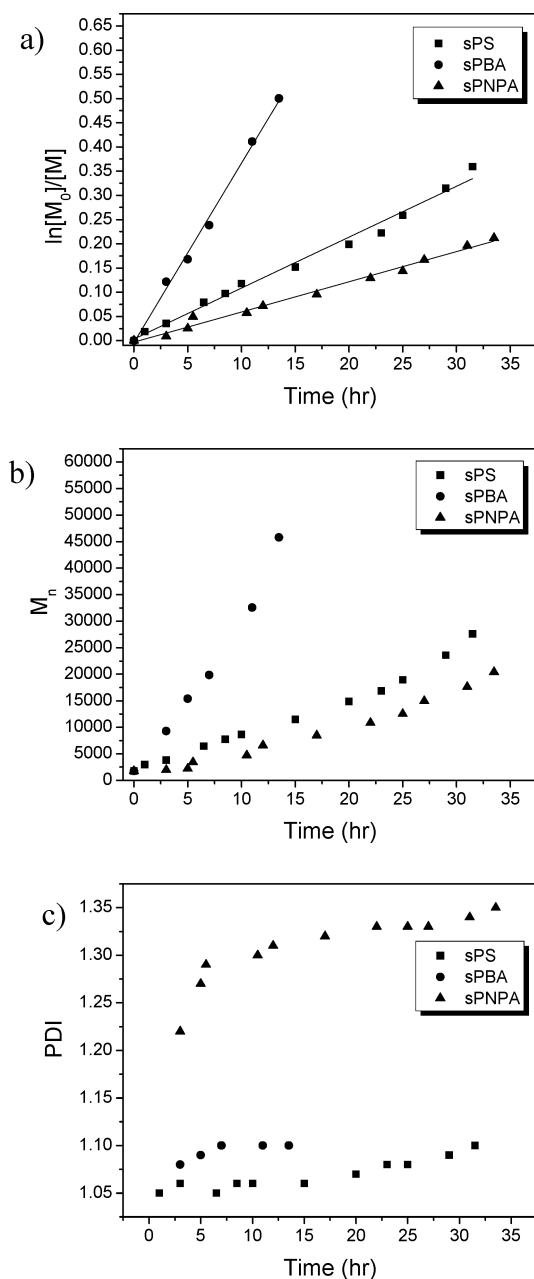


**Figure 1.** Dependence of (a)  $\ln([M]_0/[M])$ , (b)  $M_n$ , and (c) polydispersity on time in the polymerization of different monomers from T3.

leading to the similar polymerization rates in the comb-brush system.

No linear increase of molecular weight was detected during the synthesis of comb-brush polymers in contrast to the structure found in the star system. The tendency of molecular weight change throughout the polymerization process is illustrated in Figure 5. During the grafting of *tert*-butyl acrylate from the macroinitiator P3, the GPC-derived molecular weight initially appeared to increase from 88 500 to 107 700 but was followed by a dramatic decrease down to 67 900. Later, the molecular weight increased again gradually as the polymerization progressed and reached a final value of 125 700. This abnormal result may be due to the difference in hydrodynamic radii between the macroinitiator P3 and the resultant cPBA. In the first hour of polymerization, only 0.76% of *tert*-butyl

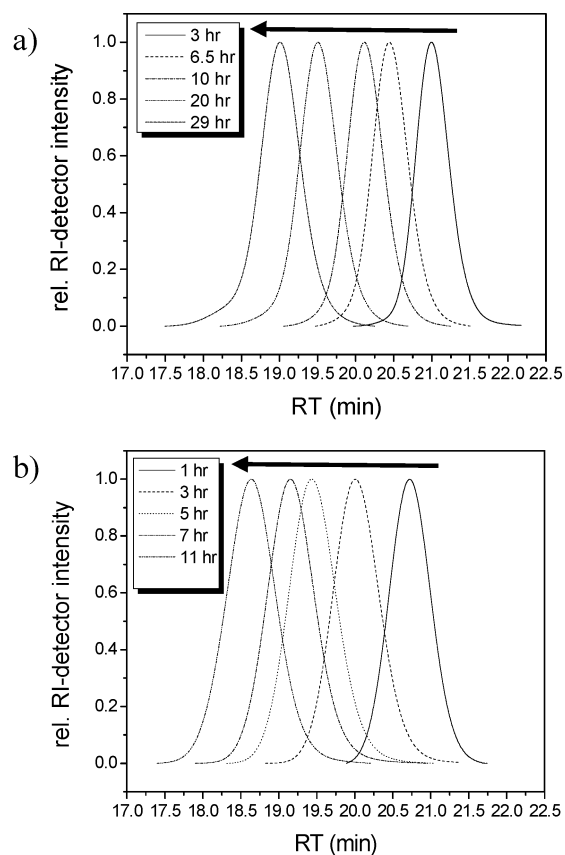


**Figure 2.** GPC traces of graft polymerization of (a) sPS and (b) sPBA from T3.

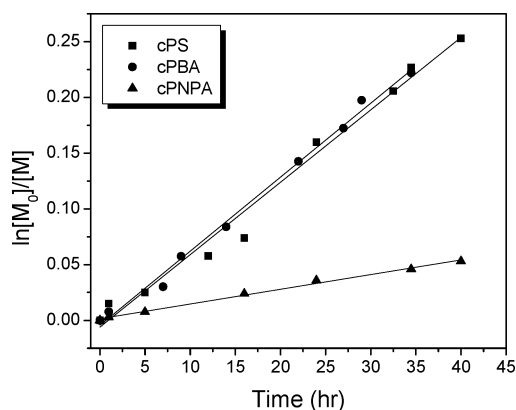


**Figure 3.** Dependence of  $\ln([M]_0/[M])$  on time in the polymerization of different monomers from P3.

acrylate was grafted onto the backbone of polyphosphazene P3. Thus, the molecular weight was still defined by the hydrodynamic radius of the polyphosphazene backbone structure, and an expected increase in molecular weight was detected by GPC. However, as more and more *tert*-butyl acrylate was grafted, the hydrodynamic radius became dominated by brush poly(*tert*-butyl acrylate) units instead of polyphosphazene, and this resulted in the initial significant decrease in measured molecular weight, followed by a gradual increase. Therefore, the actual molecular weight may be higher than the value measured by GPC. In fact, both the molecular weights calculated from conversion and from chain cleavage indicate a remarkably higher value than the one reflected by GPC (Table 2).

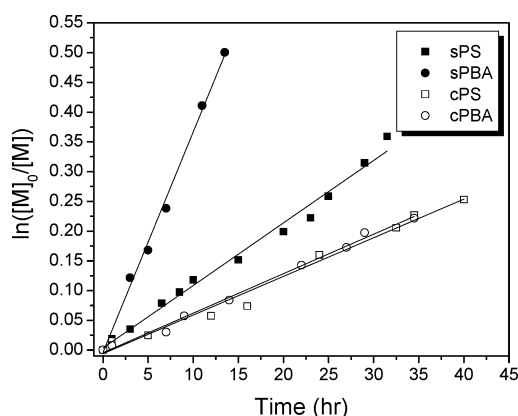


**Figure 4.** Comparison of dependence of  $\ln([M]_0/[M])$  on time in the polymerization of Sty and BA from T3 and P3.

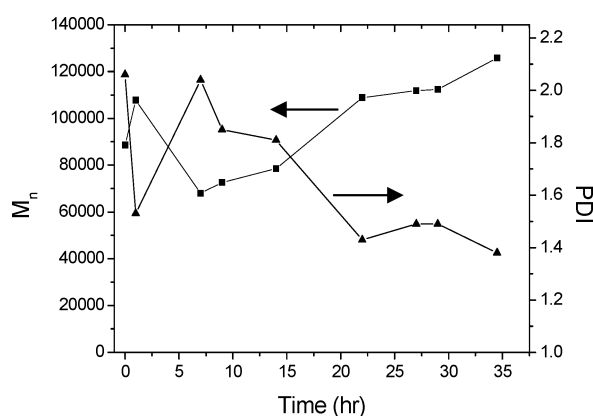


**Figure 5.** Dependence of  $M_n$  and PDI on time in the polymerization of BA from P3.

An interesting aspect is that the molecular weights of cPBA increased with polymerization time, while the molecular weight distributions decreased from 2.06 to 1.38. This decrease of the molecular weight distribution may be attributed to the formation of well-defined poly(*tert*-butyl acrylate) side chains by ATRP.<sup>53</sup> It should be pointed out that the molecular weight distribution of P3 was larger than 2 since the macroinitiators were prepared by thermal ring-opening polymerization, which usually provides no control over molecular weight distribution. In addition, all the GPC traces of the polymer brushes were found to be unimodal without any trace of a shoulder, indicating that almost all the macroinitiators were converted to the corresponding polymer brushes.

**Analysis of the Grafted Side Chains.** In order to determine the uniformity of the grafted side chains, both the star- and comb-shaped brush polymers were subjected to solvolysis to release the grafted side chains. sPS and cPS were cleaved with potassium hydroxide in THF and ethanol to release the polystyrene side chains. On the other hand, sPBA and cPBA were cleaved using acid-catalyzed transesterification in *n*-butanol to ensure that the *tert*-butyl ester groups of sPBA and cPBA side chains remained either intact or were replaced with *n*-butyl without formation of free carboxylic acid groups.

The GPC traces of the starting brush cPBA and the hydrolyzed product are given in Figure 6. The peak of the cPBA polymer disappeared after 10 days solvolysis. Instead, a low and a high molecular weight fraction appeared which confirmed the degradation of the polyphosphazene backbone and the release

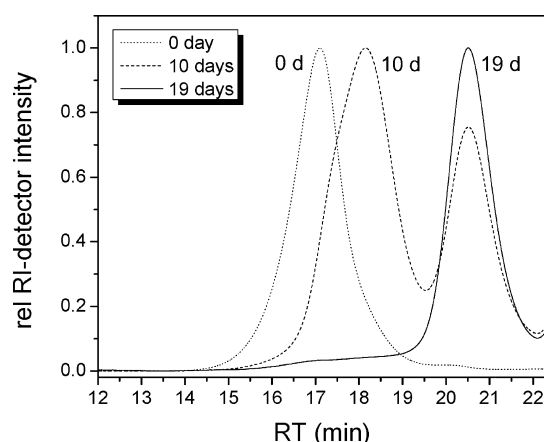


**Figure 6.** GPC traces of solvolysis of cPBA in *n*-butanol.

of the cleaved side chains, respectively. Complete cleavage required 19 days of reaction. The low molecular weight fraction has a symmetrical GPC trace, the number-average molecular weight is 5600, and the polydispersity is 1.16. Following a similar procedure, the side chains of sPBA, sPS, and cPS brush polymers were cleaved from the polymer backbones, and the low molecular weight fractions were analyzed by GPC. The results are listed in Table 3.

**Table 3.** GPC Characterization of Cleaved Brush Side Chains

	star		comb	
	sPS	sPBA	cPS	cPBA
reaction time (days)	12	12	12	19
side chain $M_n$	3001	8549	2159	5617
PDI	1.16	1.19	1.21	1.16
polymer $M_n$	19 773	53 061	862 198	2 086 330

No significant tailing of the cleaved side chains from all four brushes was detected by GPC, and the narrow unimodal distribution of the detached poly(*tert*-butyl acrylate) and polystyrene substantiates the well-controlled ATRP reaction of *tert*-butyl acrylate and styrene initiated by T3 and P3. The potential reactions that could lead to a bimodal side chain distribution such as intra- or intermolecular coupling have clearly been effectively suppressed by controlling the amount of catalyst used.

It is interesting to compare the molecular weights calculated based on the cleaved side chains with those detected by GPC (Table 2). For starlike brush polymers, no significant difference of the molecular weights was found by these two methods which is probably due to the relatively less densely grafted polymer side chains on star-shaped initiator T3 as a consequence of its relatively open conformation. However, a significant difference in molecular weight calculated by these two methods was found for comblike polymers (cPS and cPBA). As mentioned above, the probable reason is that the densely grafted and compact side chains make the hydrodynamic radius much smaller than that of the corresponding linear polymers, so the molecular weights of comblike polymers appear to be lower when compared to the molecular weights calculated from either conversion or from the cleaved side chains.

Moreover, no remaining backbone polymer was detected in the GPC traces. This may be because of the low proportion of backbone with respect to side chains or because of degradation of the polyphosphazene backbone into ammonium ion and phosphate.<sup>31,32</sup>

**Hydrolysis of sPBA/cPBA.** The brushes with PBA side chain were subjected to further functionalization in order to obtain a negatively charged polyelectrolyte.

sPBA and cPBA were treated with trimethylsilyl iodide to deprotect the *tert*-butyl ester group and form a carboxylic acid group.<sup>48,54</sup> These conditions avoid the possible cleavage of grafted side chains under harsh acidic or basic conditions. The reaction was completed within 24 h. The resultant product was 100% deprotected, as determined by <sup>1</sup>H NMR with complete disappearance of *tert*-butyl group at 1.4 ppm and was soluble in water but insoluble in tetrahydrofuran and chloroform, which is significantly different from the parent polymers, thus indicating the total cleavage of *tert*-butyl groups from the brush polymers.

**Determination of Lower Critical Solution Temperature (LCST) of cPNPA.** The lower critical solution temperature (LCST) of cPNPA was examined by both differential scanning calorimetry (DSC) and dynamic light scattering (DLS).

Figure 7a shows the enthalpy of transition of the grafted polymer cPNPA in water using DSC by repeatedly cycling the solution between 20 and 55 °C. An endothermic transition at  $32.3 \pm 0.3$  °C was detected which is assigned to the enthalpy change associated with the breaking/making of hydrogen bonds between poly(isopropylacrylamide) grafts and water.<sup>55</sup> This result is consistent with previous studies of poly(isopropylacrylamide) and confirms that the stimuli-responsive conformational change of cPNPA is reversible and sensitive to temperature variations.

In addition, the LCST and the corresponding molecular conformation transition of polymer cPNPA were also studied by DLS, which shows a change in molecular shape after passing through the LCST at 33 °C. In Figure 7b, the variations of apparent hydrodynamic radius ( $R_h$ ) and  $M_w$  with temperature are summarized. The hydrodynamic radius of brush polymer cPNPA was found to gradually decrease from 26 nm at 20 °C to 21 nm at 32.5 °C, followed by a large increase from 21 to 33 nm within a small temperature interval of 0.5 °C. The first slow decrease of  $R_h$  from 26 to 21 nm reflects the shrinkage of the individual brush polymer, where the repulsion of the densely grafted side chains represents the extension force and acts against the entropic contraction force from the phase transition due to increase of temperature. This result is similar to that reported earlier for a different system.<sup>56</sup> Afterward, the significant increase of  $R_h$  was detected beyond the LCST of cPNPA up to 34 nm, which indicates the aggregation of grafted copolymer molecules due to the enhanced hydrophobicity of poly(*N*-isopropylacrylamide).

**Synthesis of Star- and Comb-Block Copolymers.** One of the advantages of the ATRP polymerization is the preservation of chain end functionality, from which diblock or even triblock copolymers can be synthesized in a well-controlled manner.<sup>57</sup> Studies show that star polymers synthesized by ATRP also exhibit conservation of active species. Hence, it is possible to synthesize star-block copolymers by polymerization of another monomer from a preformed polymeric macroinitiator.<sup>58</sup> Therefore, both star- and comb-bush polystyrene polymers sPS and cPS were used as macroinitiators for the copper bromide/PMEDTA-mediated

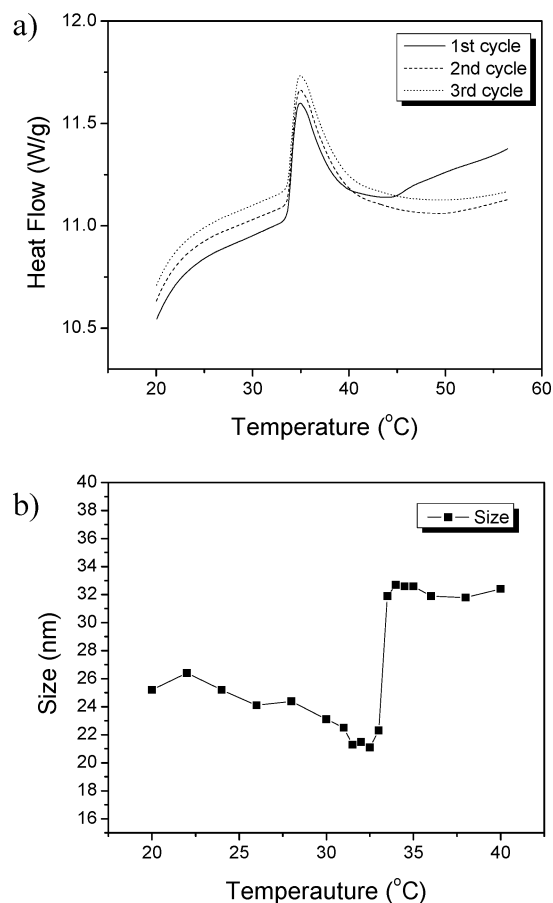


**Figure 7.** LCST of cPNAP determined by (a) DSC and (b) DLS.

polymerization of *tert*-butyl acrylate. Figure 8 illustrates GPC traces for the polymerizations of the homocopolymers (sPS) and block copolymers (sPS-*b*-PBA). The absence of a high

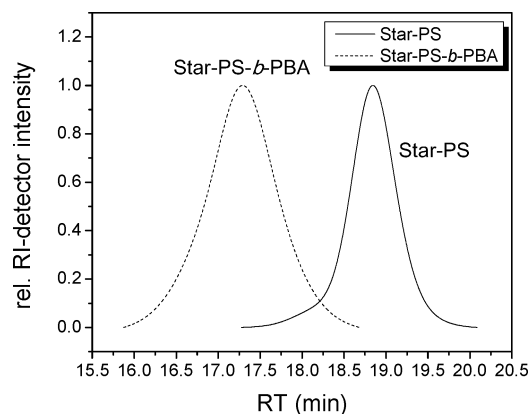


**Figure 8.** GPC traces of the subsequent synthesis of sPS-*b*-PBA.

molecular weight shoulder indicates no detectable brush-coupling product and a controlled polymerization reaction. The reaction was terminated at 61.6% conversion after 20 h for sPS-*b*-PBA. The GPC chromatograms shifted cleanly to higher molecular weight from 27 600 ( $M_w/M_n = 1.10$ ) to 107 600 ( $M_w/M_n = 1.16$ ). Furthermore, block copolymers cPS-*b*-PBA were also synthesized using cPS as a macroinitiator. The characterization data are listed in Table 4 together with sPS-*b*-PBA. Thus, a star- or comb-block copolymer consisting of a hard,

**Table 4. Molecular Weight and Polydispersity of Block Brush Copolymers**

	star		comb	
	sPS	sPS- <i>b</i> -PBA	cPS	cPS- <i>b</i> -PBA
$M_n$	27 600	107 600	200 300	435 400
PDI	1.10	1.16	1.94	1.85

high- $T_g$  segment in the core and a soft, low- $T_g$  segment in the shell was confirmed, which is a promising architecture in the design of thermoplastic elastomeric materials.

## CONCLUSIONS

A variety of well-defined, densely grafted molecular brushes based on polyphosphazenes were synthesized by ATRP polymerization. Three different monomers—styrene, *tert*-butyl acrylate, and *N*-isopropylacrylamide—have been grafted from cyclotriphosphazene or polyphosphazene initiators to form star- or comb-shaped brush polymers. Both systems follow first-order reaction kinetics during polymerization, exhibiting living polymerization features. The resultant polymers show well-defined structures with controlled molecular weight and low polydispersity. Also, the side chains, when cleaved from the skeleton, have a relatively low polydispersity,  $M_w/M_n \leq 1.21$ , which demonstrates the controlled nature of the grafting procedure. Positively charged molecular brushes were obtained through hydrolysis of *tert*-butyl groups to provide free carboxylic acid functional groups. Also, the thermal sensitivity of poly(*N*-isopropylacrylamide) brush polymers remains intact and independent of the side chain length. The interesting change of hydrodynamic radius before and after its LCST exhibits the unique properties of single cylindrical brush molecule with stimuli-responsive behavior. Furthermore, the resultant functionalized block brush polymers with a hard polystyrene core and a soft poly(*tert*-butyl acrylate) shell are promising candidates for a variety of applications in thermoplastic elastomeric materials and in the biomedical field, such as drug delivery and tissue engineering.

## AUTHOR INFORMATION

### Corresponding Author

\*E-mail: hra@chem.psu.edu.

## REFERENCES

- (1) Vanhee, S.; Rulkens, R.; Lehmann, U.; Rosenauer, C.; Schulze, M.; Kohler, W.; Wegner, G. *Macromolecules* **1996**, *29*, 5136–5142.
- (2) Khelfallah, N.; Gunari, N.; Fischer, K.; Gkogkas, G.; Hadjichristidis, N.; Schmidt, M. *Macromol. Rapid Commun.* **2005**, *26*, 1693–1697.
- (3) Neugebauer, D.; Zhang, Y.; Pakula, T.; Sheiko, S. S.; Matyjaszewski, K. *Macromolecules* **2003**, *36*, 6746–6755.
- (4) Sheiko, S. S.; Sumerlin, B. S.; Matyjaszewski, K. *Prog. Polym. Sci.* **2008**, *33*, 759–785.
- (5) Sheiko, S. S.; Moeller, M. *Chem. Rev.* **2001**, *101*, 4099–4123.
- (6) Sheiko, S. S.; da Silva, M.; Shirvanyants, D.; LaRue, I.; Prokhorova, S.; Moeller, M.; Beers, K.; Matyjaszewski, K. *J. Am. Chem. Soc.* **2003**, *125*, 6725–6728.
- (7) Panyukov, S.; Zhulina, E. B.; Sheiko, S. S.; Randall, G. C.; Brock, J.; Rubinstein, M. *J. Phys. Chem. B* **2009**, *113*, 3750–3768.
- (8) Park, I.; Sheiko, S. S.; Nese, A.; Matyjaszewski, K. *Macromolecules* **2009**, *42*, 1805–1807.
- (9) Djalali, R.; Li, S. Y.; Schmidt, M. *Macromolecules* **2002**, *35*, 4282–4288.

- (10) Zhang, M. F.; Breiner, T.; Mori, H.; Muller, A. H. E. *Polymer* **2003**, *44*, 1449–1458.
- (11) Li, C. M.; Gunari, N.; Fischer, K.; Janshoff, A.; Schmidt, M. *Angew. Chem., Int. Ed.* **2004**, *43*, 1101–1104.
- (12) Cheng, C.; Qi, K.; Khoshdel, E.; Wooley, K. L. *J. Am. Chem. Soc.* **2006**, *128*, 6808–6809.
- (13) Huang, K.; Rzayev, J. *J. Am. Chem. Soc.* **2009**, *131*, 6880–6885.
- (14) Tang, C.; Dufour, B.; Kowalewski, T.; Matyjaszewski, K. *Macromolecules* **2007**, *40*, 6199–6205.
- (15) Iozzo, R. V. *Proteoglycans: Structure, Biology, and Molecular Interactions*; Marcel Dekker: New York, 2000.
- (16) Varki, A.; Cummings, R.; Esko, J.; Freeze, H.; Hart, G.; Marth, J. *Essentials of Glycobiology*; Cold Spring Harbor Laboratory Press: Cold Spring Harbor, NY, 1999.
- (17) Kaneider, N. C.; Duzendorfer, S.; Wiedermann, C. J. *Biochemistry* **2004**, *43*, 237–244.
- (18) Scott, J. E. *Biochemistry* **1996**, *35*, 8795–8799.
- (19) Khalsa, P. S.; Eisenberg, S. R. *J. Biomech.* **1996**, *30*, 589–594.
- (20) Bromberg, L. E.; Barr, D. P. *Biomacromolecules* **2000**, *1*, 325–334.
- (21) Deffieux, A.; Schappacher, M. *Macromolecules* **1999**, *32*, 1797–1802.
- (22) Sumerlin, B. S.; Neugebauer, D.; Matyjaszewski, K. *Macromolecules* **2005**, *38*, 702–708.
- (23) Tsarevsky, N. V.; Matyjaszewski, K. *Chem. Rev.* **2007**, *107*, 2270–2299.
- (24) Heroguez, V.; Breunig, S.; Gnanou, Y.; Fontanille, M. *Macromolecules* **1996**, *29*, 4459–4464.
- (25) Balamurugan, S. S.; Bantchev, G. B.; Yang, Y. M.; McCarley, R. L. *Angew. Chem., Int. Ed.* **2005**, *44*, 4872–4876.
- (26) Wang, M. F.; Zou, S.; Guerin, G.; Shen, L.; Deng, K. Q.; Jones, M.; Walker, G. C.; Scholes, G. D.; Winnik, M. A. *Macromolecules* **2008**, *41*, 6993–7002.
- (27) Yokoyama, M. *J. Artif. Organs* **2005**, *8*, 77–84.
- (28) Allcock, H. R.; Connolly, M. S.; Sisko, J. T.; Alshali, S. *Macromolecules* **1988**, *21*, 323–334.
- (29) Gleria, M.; Bolognesi, A.; Porzio, W.; Catellani, M.; Destri, S.; Audisio, G. *Macromolecules* **1987**, *20*, 469–473.
- (30) Allcock, H. R.; Nelson, C. J.; Coggio, W. D. *Organometallics* **1991**, *10*, 3819–3825.
- (31) Krogman, N. R.; Singh, A.; Nair, L. S.; Laurencin, C. T.; Allcock, H. R. *Biomacromolecules* **2007**, *8*, 1306–1312.
- (32) Deng, M.; Nair, L. S.; Nukavarapu, S. P.; Kumbar, S. G.; Jiang, T.; Krogman, N. R.; Singh, A.; Allcock, H. R.; Laurencin, C. T. *Biomaterials* **2008**, *29*, 337–349.
- (33) Wisian-Neilson, P.; Schaefer, M. A. *Macromolecules* **1989**, *22*, 2003–2007.
- (34) Allcock, H. R.; de Denus, C. R.; Prange, R.; Laredo, W. R. *Macromolecules* **2001**, *34*, 2757–2765.
- (35) Prange, R.; Reeves, S. D.; Allcock, H. R. *Macromolecules* **2000**, *33*, 5763–5765.
- (36) Korsak, V. V.; Vinogradova, S. V.; Tur, D. R.; Gilman, L. M. *Acta Polym.* **1980**, *31*, 85–9.
- (37) Allcock, H. R.; Kuharcik, S. E.; Reed, C. S.; Napierala, M. E. *Macromolecules* **1996**, *29*, 3384–3389.
- (38) Chang, J. Y.; Park, P. J.; Han, M. J. *Macromolecules* **2000**, *33*, 321–325.
- (39) Gleria, M.; Minto, F.; Scoptoni, M.; Pradella, F.; Carassiti, V. *Chem. Mater.* **1992**, *4*, 1027–1032.
- (40) Minto, F.; Gleria, M.; Bortolus, P.; Fambri, L.; Pegoretti, A. *J. Appl. Polym. Sci.* **1995**, *56*, 747–756.
- (41) Matyjaszewski, K.; Miller, P. J.; Pyun, J.; Kickelbick, G.; Diamanti, S. *Macromolecules* **1999**, *32*, 6526–6535.
- (42) Liu, W.; Jin, J.; Huang, X.; Zheng, Y.; Zhang, J.; Fu, J.; Huang, Y.; Tang, X. *Polym. Int.* **2010**, *59*, 1252–1257.
- (43) Cambre, J. N.; Wisian-Neilson, P. *J. Inorg. Organomet. Polym. Mater.* **2006**, *16*, 311–318.
- (44) Matyjaszewski, K.; Miller, P. J.; Fossum, E.; Nakagawa, Y. *Appl. Organomet. Chem.* **1998**, *12*, 667–673.

- (45) Pangborn, A. B.; Giardello, M. A.; Grubbs, R. H.; Rosen, R. K.; Timmers, F. J. *Organometallics* **1996**, *15*, 1518–1520.
- (46) Britovsek, G. J. P.; England, J.; White, A. J. P. *Inorg. Chem.* **2005**, *44*, 8125–8134.
- (47) Allcock, H. R.; Kugel, R. L.; Valan, K. J. *Inorg. Chem.* **1966**, *5*, 1709–1715.
- (48) Jung, M. E.; Lyster, M. A. *J. Am. Chem. Soc.* **1977**, *99*, 968–969.
- (49) Ueda, J.; Kamigaito, M.; Sawamoto, M. *Macromolecules* **1998**, *31*, 6762–6768.
- (50) Cheng, G. L.; Boker, A.; Zhang, M. F.; Krausch, G.; Muller, A. H. E. *Macromolecules* **2001**, *34*, 6883–6888.
- (51) Borner, H. G.; Duran, D.; Matyjaszewski, K.; da Silva, M.; Sheiko, S. S. *Macromolecules* **2002**, *35*, 3387–3394.
- (52) Fischer, H. *Macromolecules* **1997**, *30*, 5666–5672.
- (53) Ding, L.; Huang, Y. Y.; Zhang, Y. Y.; Deng, J. P.; Yang, W. T. *Macromolecules* **2011**, *44*, 736–743.
- (54) Liu, G. J.; Ding, J. F. *Adv. Mater.* **1998**, *10*, 69–70.
- (55) Heskins, J.; Guillet, E. J. *Macromol. Sci., Part A: Chem.* **1968**, *2*, 1441–1455.
- (56) Fischer, K.; Schmidt, M. *Macromol. Rapid Commun.* **2001**, *22*, 787–791.
- (57) Borner, H. G.; Beers, K.; Matyjaszewski, K.; Sheiko, S. S.; Moller, M. *Macromolecules* **2001**, *34*, 4375–4383.
- (58) Strandman, S.; Zarembo, A.; Darinskii, A. A.; Lauritnaki, P.; Butcher, S. J.; Vuorimaa, E.; Lemmetyinen, H.; Tenhu, H. *Macromolecules* **2008**, *41*, 8855–8864.